British Columbia Geological Survey

Open File 2020-04

Geology of the Polaris Alaskan-type ultramafic-mafic intrusion, north-central British Columbia

parts of NTS 94C/12 and 05

Sheet 2 of 2

James A. Nott*, Dejan Milidragovic**, Graham T. Nixon**, James S. Scoates*

*Pacific Centre for Isotopic and Geochemical Research, University of British Columbia, ** British Columbia Geological Survey

0 0.25 0.5 1 1.5 2 Kilometres

Scale 1:15,000

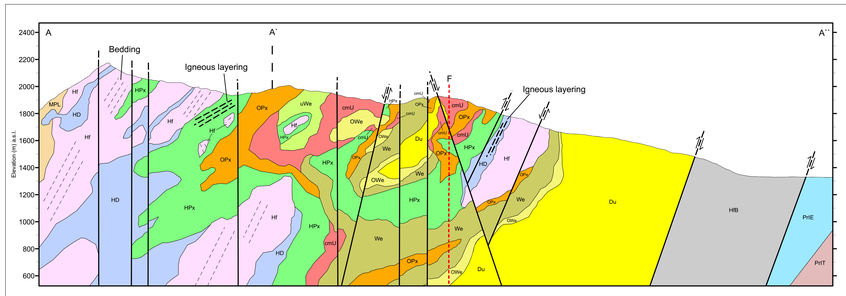

Cross-Section Notes

Scale 1:15,000
No vertical exaggeration, elevation in metres above sea level (a.s.l.)

Dashed red lines on F-F'' represent the depth of intersecting (A-E) cross section. Intersection of F-F'' is noted on A-E sections. Change of strike direction of a cross section is noted by a dashed black line above surface at respective locations.

These cross sections are schematic interpretations of subsurface geology partly constrained by field observations, geophysical data, and the distribution of units in the vicinity of the section exposed at different topographic elevations. Certain minor features observed in outcrop are represented in the cross-sections to illustrate intrusive relationships and structural attitudes. (e.g., late-stage felsic dikes, cross-cutting HPx and HD dikes, bedding, and igneous layering).

Evidence of remobilized chromitites, magmatic breccias, and chaotically intermingled units suggests multiple intrusive phases throughout the intrusion's protracted evolution. Periodic episodes of magma intrusion and infiltration have disrupted the gross primary cumulate sequence.

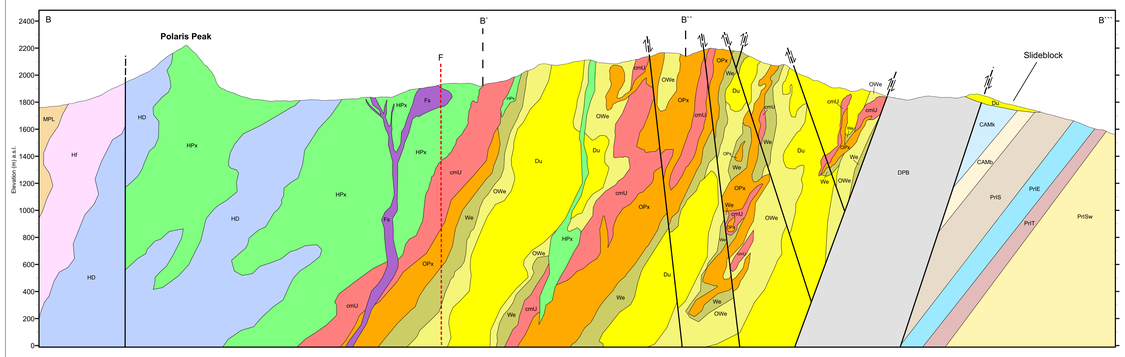

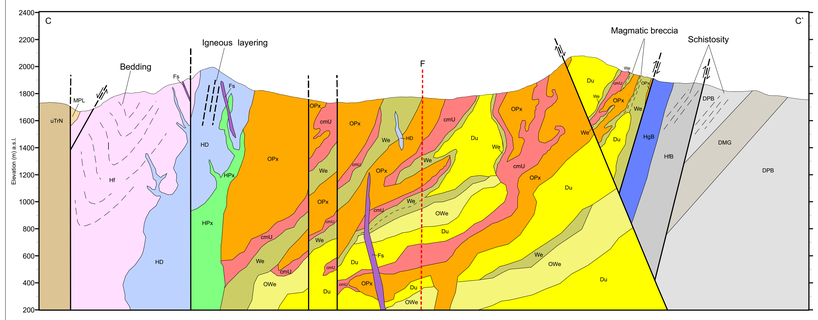

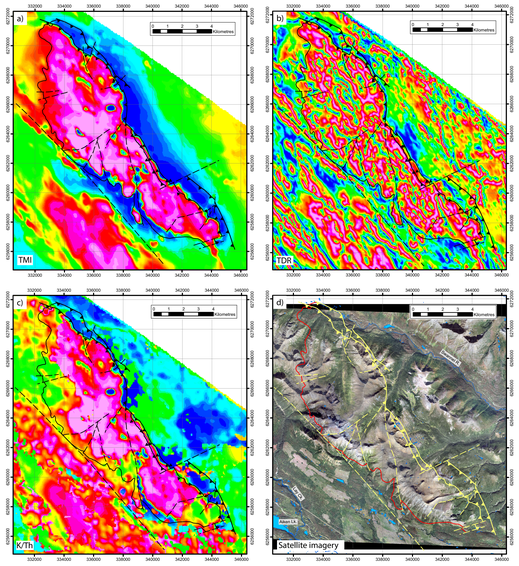

Fig. 2. Remote sensing images of the Polaris intrusion. **a)** Total magnetic intensity (TMI) map; **b)** Magnetic tilt derivative (TDR) map; **c)** K/Th radiometric map; **d)** Virtual Earth satellite photograph. Geophysical data in panels a-c is represented by pink=high and blue=low values; acquired from CGG, Canada Services Ltd. (2018). UTM Zone 10, NAD83.

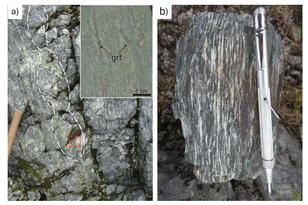

Fig.3. Metamorphosed contact rocks of eastern margin. **a)** Strongly foliated metavolcanic (?) rock with garnet-bearing boudins. Inset of cut sample, showing fine- to medium-grained garnet porphyroblasts. **b)** Mylonitic gabbro typical along eastern thrust fault contact (HgB). Scales: hammer handle, 5 cm wide; pen, 13 cm long and 1 cm wide. Contacts: approximate, dashed. Photograph locations (UTM Zone 10, NAD83): a) 339004m E, 6263548m N; b) 337528m E, 6267681m N.

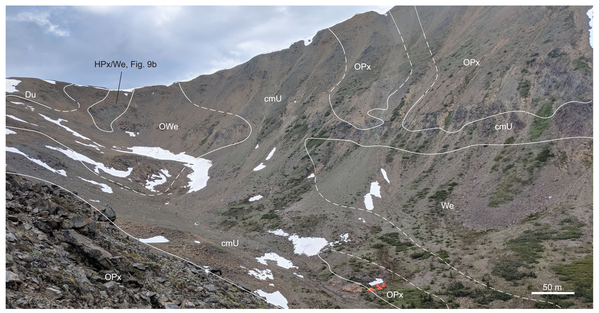

Fig. 6. View looking west (see map for location) illustrating the typical irregular contacts between a chaotic intermingled unit (cmU) and olivine clinopyroxenite (OPx), olivine wehrlite (OWe), wehrlite (We), and dunite (Du). Location of photograph in Fig. 9b is shown. Note orange tents for scale along floor of valley. Contacts: observed, solid line; approximate, dashed line. Photograph location (UTM Zone 10, NAD83): 337690m E, 6265700m N.

Geological Summary

The Early Jurassic Polaris Alaskan-type ultramafic-mafic intrusion is approximately 200 km northeast of Smithers in north-central British Columbia, in the Lay Range of the Omineca Mountains. The intrusion belongs to a global class of convergent margin ultramafic-mafic intrusions known as 'Alaskan-type' that are characterized by a lack of orthopyroxene throughout (Irvine, 1974b; Nixon et al., 2015). The Polaris intrusion is one of the best exposed Alaskan-type ultramafic-mafic bodies in the Canadian Cordillera, second in size only to the Tulameen intrusion in south-central British Columbia (Fig. 1; Nixon et al., 2018). New detailed (≤1:15,000) field mapping and lithological sampling integrated with the results of a recent aeromagnetic survey (Fig. 2, CGG Canada Services Ltd., 2018) has enabled refinement of internal and external geological relationships and established an intrusion-wide geochronological sample set.

Emplacement of the Polaris intrusion (ca. 186 Ma, Nixon et al., 2019) was coeval with emplacement of the Turnagain Alaskan-type intrusion, which occupies a similar structural setting in the Yukon-Tanana terrane (ca. 189-185 Ma, Nixon et al., 2020a; Fig. 1). Intrusion of these Alaskan-type bodies was synchronous with contractional deformation marking the initial accretion of peri-Laurentian arc terranes to the continental margin in the Early Jurassic (Nelson et al., 2013; Monger and Gibson, 2019; Nixon et al., 2020a). The Polaris intrusion (45 km^2) forms a discordant sill-like body (14 km long, up to 3 km wide) that is hosted by westward-dipping (30-50°) late Paleozoic (Mississippian-Permian) metamorphosed arc-derived mafic-intermediate volcanic breccias, flows, and sedimentary strata of the Lay Range assemblage (Quesnel terrane) (Roots, 1954, Nixon et al., 1997, Nott et al., 2020). The intrusion is in thrust contact with Late Devonian to Permian rocks of the ancestral continental margin of North America to the east.

The metamorphic contact aureole in the volcano-sedimentary host rocks is greenschist to lower amphibolite facies, and locally exhibits an amphibole lineation and foliation. The presence of andalusite in the southern and eastern contact aureole constrains the depth of emplacement of the Polaris intrusion to less than 12 km (Nixon et al., 1997). Along parts of its eastern margin, the intrusion is in thrust contact with variably foliated to non-foliated gabbro-diorite, and locally hornfelsed host rocks of the Big Creek group (Figs. 3, 4a, c; Nott et al., 2020).

Ultramafic-mafic rock types forming the Polaris intrusion are distributed asymmetrically and represent a crude internal stratigraphy. Dunite (with minor chromitite) is predominant in the eastern part of the intrusion, olivine clinopyroxenite is prevalent in the central portion, and hornblende-bearing gabbro-diorite and pyroxenite are largely restricted to the 'roof zone' in the west. A narrow belt of zoned ultramafic cumulates is locally preserved along the eastern thrust margin and passes (east to west) from olivine clinopyroxenite through wehrlite and olivine wehrlite to dunite (Fig. 4). This zonation appears to have developed at the intrusive contact with the Lay Range assemblage, which has been removed by faulting. Although cumulate textures characterize the ultramafic and mafic rocks, cm-scale magmatic modal layering (Fig. 5) is rare. Mappable zones of chaotically intermingled ultramafic cumulates (cmU) locally disrupt the gross internal stratigraphy (Figs. 6, 7), and remobilized chromitite schlieren are dispersed throughout the dunite (Fig. 8). The cmU zones and remobilized chromitite may be related to episodic magma replenishment within the crustal magma chamber (Nixon et al., 2020b).

Contacts between rock types are commonly irregular and vary from sharp to gradational or diffuse and can be divided into two main categories: 1) contacts formed by the products of fractional crystallization and accumulation during progressive magmatic differentiation; and 2) contacts between these rocks and chaotically intermingled ultramafic cumulates (cmU). The decametre- to metre-scale intermingling is prominent near the margins of clinopyroxenite and wehrlite units and, less commonly, dunite. The textural and intrusive relationships in the chaotically intermingled units (Figs. 6, 7, 9) indicate both ductile and brittle behaviour of variably consolidated ultramafic cumulates in differing thermal and/or rheological states (Nott et al., 2020).

Local orthomagmatic sulphides (pyrrhotite, pentlandite, chalcopyrite, pyrite, and rare bornite) are predominantly in clinopyroxene- and hornblende-rich rocks, although they also occur in wehrlite and gabbro-diorite. The mineralized rocks commonly weather reddish to rusty brown and display prominent malachite staining. The magmatic composition and textures of the sulphides are evident from ovoid inclusions of a formerly immiscible sulphide melt enclosed in clinopyroxene and hornblende primocrysts, and irregular films and pockets of interstitial sulphides trapped within the cumulate silicate framework (Fig. 10). The disseminated to locally blebby sulphides may constitute up to 15-20 vol. % of mineralized samples (Nixon et al., 2020b). Whole rock analysis of chalcopyrite-bearing samples from a number of mineralized zones have maximum values of 1.18 wt. % Cu, 1.8 g/t Pd and 1.3 g/t Pt with Pd/Pt = 1.4 (Mowat, 2015).

Ongoing petrochronological research and high-precision geochronology aim to develop a detailed emplacement framework for the Polaris intrusion using U-Th-Pb-bearing accessory minerals (e.g., zircon, titanite) to constrain the timing of mineralization, intrusion formation, and physicochemical environment of this Alaskan-type intrusion.

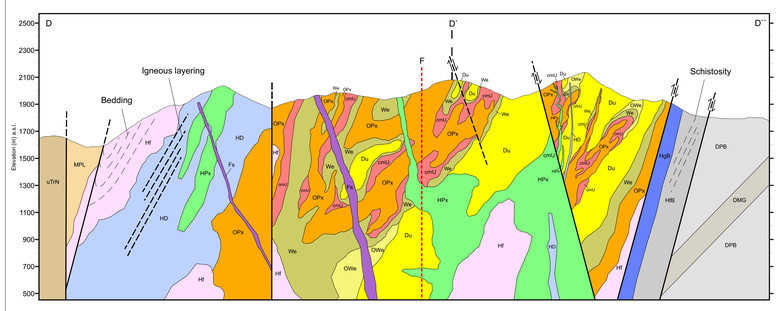

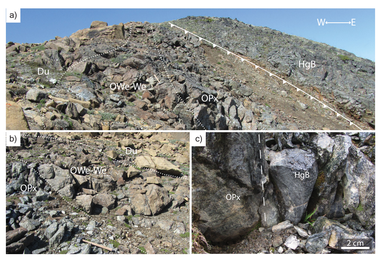

Fig. 4. Contact relationships in the eastern part of the Polaris intrusion (see map for location). **a)** Footwall gabbro (HgB) in thrust contact with olivine clinopyroxenite (OPx) that grades, from east to west, into olivine wehrlite to wehrlite (OWe-We) and dunite (Du). View looking north. **b)** M-scale gradational contacts of olivine clinopyroxenite, olivine wehrlite to wehrlite, and dunite. **c)** Undeformed coarse-grained (≤5 mm) olivine clinopyroxenite in thrust contact with mylonitic gabbro in the footwall. Scale: hammer is 40cm long, head 5 cm wide. Contacts: gradational, dotted line; observed/approximate, solid/dashed line. Photograph locations (UTM Zone 10, NAD83): a) 339122m E, 6263234m N; b) 339058m E, 6263306m N; c) 339463m E, 6262727m N.

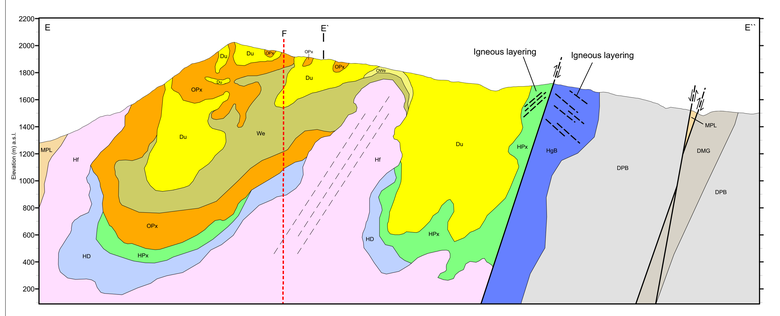

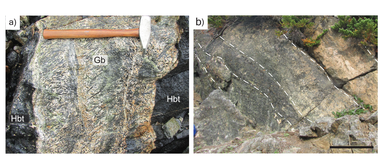

Fig. 5. Hornblende-bearing rocks. **a)** Hornblende gabbro dike (Gb) with internal dike-parallel layering. Prismatic hornblende crystals (≤ 10 cm long) with long axes at high angles to the sharp external contact with massive pegmatitic hornblendite (Hbt) containing interstitial feldspar. **b)** Magmatic layering in coarse-grained to pegmatitic (≤15 cm) hornblendite to gabbro (Hbt). Scale: hammer is 40cm long, head is 5 cm wide. Photograph locations (UTM Zone 10, NAD83): a) 334830m E, 6264325m N; b) 333203m E, 6267766m N.

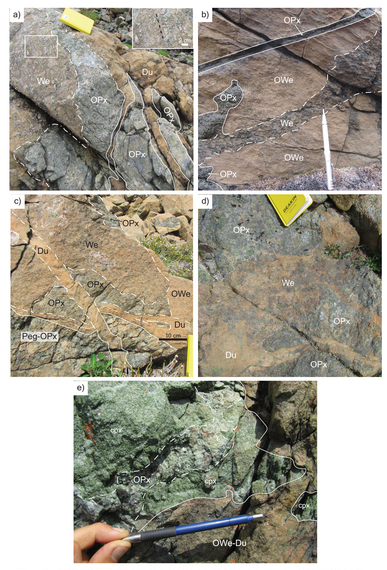

Fig. 7. Textural and lithological relationships in the chaotic intermingled units (cmU). **a)** Coarse-grained olivine clinopyroxenite (OPx) blocks in wehrlite (We), cut by fine-grained dunite dikes (Du). Inset illustrates alignment (dashed line) of subhedral to euhedral clinopyroxene crystals (3-4 cm) in wehrlite. **b)** Olivine wehrlite (OWe) with coarse-grained olivine clinopyroxenite (OPx) cut by coarse-grained (<5 mm clinopyroxene) wehrlite (We) with diffuse contacts. Clinopyroxene clusters in wehrlite are ~15 mm across and olivine-rich pods have similar textures (equigranular) and grain size as host. **c)** Complex relationships among dunite (Du), olivine wehrlite (OWe), wehrlite (We), and locally pegmatitic (Peg-OPx) olivine clinopyroxenite (OPx). Offset of dunite dike delineated by fine-dashed line. **d)** Heterogeneous zone consisting of dunite (Du) showing gradational boundaries with wehrlite (We) and diffuse to sharp boundary with blocks of olivine clinopyroxenite (OPx). **e)** Granular, equant, anhedral crystals (<1 mm) of bright green clinopyroxene (cpx) intergrown with coarse-grained (2-5 mm) olivine clinopyroxenite (OPx) in olivine wehrlite-dunite (OWe-Du). Contacts: diffuse, dot-dash line; sharp, solid line. Photograph locations (UTM Zone 10, NAD83): a) 336573m E, 6266640m N; b) 337327m E, 6265429m N; c) 337554m E, 6265572m N; d) 337989m E, 6262932m N; e) 334152m E, 6268605m N.

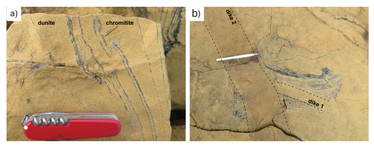

Fig. 8. Chromitite schlieren. **a)** Ductile deformation of adcumulate dunite containing thin laminae of chromitite and showing an isolated fold. **b)** Fragment of layered chromitite cut by two generations of dunite (1) and wehrlite (2) dikes (dashed outline), illustrating early ductile deformation and fragmentation of layered chromitite-dunite followed by late injection of dunite and wehrlite into a consolidated brittle host. Photograph locations (UTM Zone 10, NAD83): a) 340659m E, 6259242m N; b) 341144m E, 6259320m N.

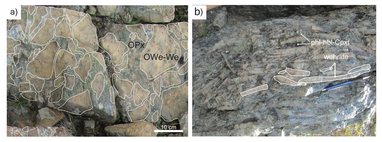

Fig. 9. Magmatic breccia. **a)** Angular to rounded blocks of olivine wehrlite-wehrlite (OWe-We) with sharp to weakly gradational boundaries (solid line) set in a groundmass of medium-grained olivine clinopyroxenite (OPx). **b)** Angular to subangular tabular xenoliths of wehrlite in a coarse-grained phlogopite-hornblende-bearing clinopyroxenite groundmass (phl-hbl-Cpxt). See Fig. 6 for location. Scale: pencil is 15 cm long, 1 cm wide. Photograph locations (UTM Zone 10, NAD83): a) 338724m E, 6263569m N; b) 336813m E, 6265478m N.

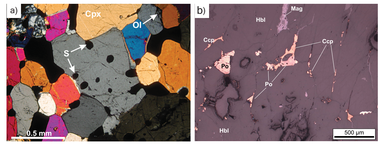

Fig. 10. Photomicrographs of sulphides in the Polaris intrusion. **a)** Cross-polarized transmitted light image of disseminated magmatic sulphides in olivine-bearing clinopyroxenite. The rounded shapes of sulphide inclusions in clinopyroxene and along silicate grain boundaries indicate trapping of immiscible sulphide liquid during silicate crystallization and accumulation. **b)** Reflected light image of primary and remobilized, fracture-filling sulphides in hornblendite. Abbreviations: S, undifferentiated sulphide; Ccp, chalcopyrite; Cpx, clinopyroxene; Hbl, hornblende; Mag, magnetite; Ol, olivine; Pn, pentlandite; Po, pyrrhotite. Scales as noted on each panel.

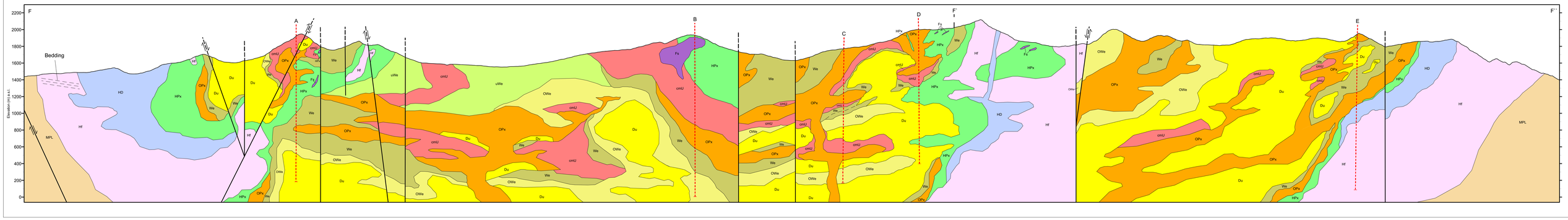

References cited

CGG Canada Services Ltd., 2018. Geophysical survey report MIDAS high resolution magnetic and radiometric survey Search Project Phase III. Geoscience BC Report 2018-2.

Ferri, F., Dudka, S., Rees, C., and Meldrum, D., 2001. Geology of the Aiken Lake Area, North-Central British Columbia, B.C. Ministry of Energy and Mines, Geoscience Map 2001-10, 1:50,000 scale.

Irvine, T.N., 1974b. Petrology of the Duke Island ultramafic complex, southeastern Alaska; Geological Society of America Memoir 138, 240 p.

Monger, J.W.H. and Gibson, H.D., 2019. Mesozoic-Cenozoic deformation in the Canadian Cordillera: The record of a "Continental Bulldozer"? Tectonophysics, 757, 153–169.

Mowat, U., 2015. Sampling on the Star 1, 3, 8, 10, 11 and 12 claims, British Columbia Ministry of Energy, Mines and Petroleum Resources, British Columbia Geological Survey Assessment Report 35680, 88p.

Nelson, J., Colpron, M., and Israel, S., 2013. The Cordillera of British Columbia, Yukon and Alaska: tectonics and metallogeny. In: Colpron, M., Bissig, T., Rusk, B., and Thompson, J.F.H., (Eds.), Tectonics, Metallogeny, and Discovery - the North American Cordillera and Similar Accretionary Settings. Society of Economic Geologists Special Publication 17, pp. 53-109.

Nixon, G. T., Hammack, J. L., Ash, C. H., Cabri, L. J., Case, G., Connelly, J. N., Hearman, L., Laflamme, J. H. G., Nuttall, C., Paterson, W. P. E., and Wong, R. H., 1997. Geology and platinum-group-element mineralization of Alaskan-type ultramafic-mafic complexes in British Columbia. British Columbia Ministry of Employment and Investment, British Columbia Geological Survey Bulletin 93, 142p.

Nixon, G.T., 2018. Geology of the Tulameen Alaskan-type ultramafic-mafic intrusion, British Columbia, scale 1:20,000. British Columbia Ministry of Energy, Mines and Petroleum Resources, British Columbia Geological Survey Open File 2018-02, 1:20,000-scale.

Nixon, G.T., Manor, M.J., Jackson-Brown, S., Scoates, J.S., and Ames, D.E., 2015. Magmatic Ni-Cu-PGE sulphide deposits at convergent margins. In: Targeted Geoscience Initiative 4: Canadian nickel-copper-platinum group elements-chromium ore systems - fertility, pathfinders, new and revised models. Geological Survey of Canada Open File 7856, pp. 19–34.

Nixon, G. T., Milidragovic, D., and Scoates, J. S., 2019. Convergent margin Ni-Cu-PGE-Cr ore systems: temporal and magmatic evolution. In: Targeted Geoscience Initiative 5, Grant Program Interim Reports 2018-2019. Geological Survey of Canada Open File 8620, pp. 49–61.

Nixon, G.T., Scheel, J.E., Scoates, J.S., Friedman, R.M., Wall, C.J., Gabites, J., and Jackson-Brown, S., 2020a. Syn-accretionary multistage assembly of an Early Jurassic Alaskan-type intrusion in the Canadian Cordillera: U-Pb and 40Ar/39Ar geochronology of the Turnagain ultramafic-mafic intrusive complex, Yukon-Tanana terrane. Canadian Journal of Earth Sciences, 57, 575–600.

Nixon, G. T., Scoates, J. S., Milidragovic, D., Nott, J., Moerhuis, N., Van Hoeve, T. J., Manor, M. J., Kjarsgaard, I. M., 2020b. Convergent margin Ni-Cu-PGE-Cr ore systems: U-Pb petrochronology and environments of Cu-PGE vs Cr-PGE mineralization in Alaskan-type intrusions. Geological Survey of Canada Open File 8722 (in press).

Nott, J., Milidragovic, D., Nixon, G.T., and Scoates, J.S., 2020. New geological investigations of the Early Jurassic Polaris ultramafic-mafic Alaskan-type intrusion, north-central British Columbia. In: Geological Fieldwork 2019, British Columbia Ministry of Energy, Mines, and Petroleum Resources, British Columbia Geological Survey Paper 2020-01, pp. 59–76.

Roots, E. F., 1954. Geology and mineral deposits of Aiken Lake map-area, British Columbia. Geological Survey of Canada Memoir 274, 246p.